Programs and Algorithms of Numerical Matematics 16
J. Chleboun, K. Segeth, J. Šístek, T. Vejchodský (Eds.)
Institute of Mathematics AS CR, Prague 2013

ON ESTIMATION OF DIFFUSION COEFFICIENT BASED ON SPATIO-TEMPORAL FRAP IMAGES: AN INVERSE ILL-POSED PROBLEM

Radek Kaňa[1], Ctirad Matonoha[2], Štěpán Papáček[3], Jindřich Soukup[3]

[1] Institute of Microbiology,
Academy of Sciences of the Czech Republic
Opatovický mlýn, 379 81 Třeboň, Czech Republic
kana@alga.cz
[2] Institute of Computer Science,
Academy of Sciences of the Czech Republic
Pod Vodárenskou věží 2, 182 07 Prague 8, Czech Republic
matonoha@cs.cas.cz
[3] University of South Bohemia in České Budějovice, Faculty of Fisheries and Protection of Waters, CENAKVA, School of Complex Systems, Zámek 136, 373 33 Nové Hrady, Czech Republic
spapacek@frov.jcu.cz, jindra@matfyz.cz

Abstract

We present the method for determination of phycobilisomes diffusivity (diffusion coefficient D) on thylakoid membrane from fluorescence recovery after photobleaching (FRAP) experiments. This was usually done by analytical models consisting mainly of a simple curve fitting procedure. However, analytical models need some unrealistic conditions to be supposed. Our method, based on finite difference approximation of the process governed by the Fickian diffusion equation and on the minimization of an objective function representing the disparity between the measured and simulated time-varying fluorescent particles concentration profiles, naturally accounts for experimentally measured time-varying Dirichlet boundary conditions and can include a reaction term as well. The result we get is the overall (time averaged) diffusion coefficient D and the sequence of diffusivities D_j based on two successive fluorescence profiles in *j-th* time interval. Due to the ill-posedness of our inverse problem, regularization algorithms are implemented. On the synthetic example, we illustrate the behaviour of solution depending on regularization parameter for different signal to noise ratio.

1. Introduction

Fluorescence Recovery After Photobleaching (FRAP) measuring technique is widely used since 1970s to study the organization and dynamics of many photosynthetic pigment-protein complexes in the photosynthetic membrane [16]. Later

on, FRAP has been extended to the investigation of protein dynamics within the living cells [14]. Using fluorescence confocal microscopy we get the spatio-temporal FRAP images, and consequently the mobility of photosynthetic complexes in a native intact membrane, i.e. the diffusivity or diffusion coefficient D,[1] is reconstructed using either a *closed form model* or *simulation based model* [9, 6]. The FRAP images are in general very noisy, with small signal to noise ratio (SNR), which requires an adequate technique assuring the reliable results.[2]

Our study describes the development of a method aiming to determine the phycobilisomes diffusivity on thylakoid membrane from FRAP experiments. As we know, this is usually done by experimental curve fitting to the analytical (closed form) models, see e.g. [1, 10, 7, 15]. However, the closed form models need some unrealistic assumptions. For example, C. W. Moulineaux *et al.* [10] have exploited the rotational symmetry of the cells by bleaching a plane across the short axis of the cell and reaching one-dimensional bleaching profiles along the long axis. Moreover, it was supposed that: (i) $x \in \mathcal{R}$, i.e. the infinite domain, (ii) the initial bleaching profile is Gaussian, and (iii) the recovery is complete for $t \to \infty$.[3] The calculation of diffusion coefficient D then resides in the weighted linear regression. The error analysis for this method, i.e. how the noise corrupts the result, we treat in paper [13].

As the analytical approach has several limitation (e.g. restriction to the specific cell geometry, bleach profile must be gaussian-like, full recovery is required, etc.), we model the FRAP process by the Fickian diffusion equation with realistic initial and boundary conditions instead. The estimation of diffusivity is further formulated as a single parameter optimization problem consisting in the minimization of an objective function representing the disparity between the experimental and simulated time-varying concentration profiles.

The paper is organized as follows. The model of the process (i.e. reaction-diffusion system) and the real data form we deal with are introduced in the second section. In the third section we define the optimization problem, describe a regularization method and its implementation. The results of the numerical simulations are contained in the fourth section, while in the fifth section the paper is concluded.

---

[1] I. F. Sbalzarini in [14] distinguishes between the molecular diffusion constant and the apparent diffusion constant; while the former is directly measured by single-molecule techniques, the latter is determined by coarse-grained methods such as FRAP, averaging over a certain observation volume.

[2] Let us mention that the fluorescence confocal microscope allows the selection of a thin cross-section of the sample by rejecting the information coming from the out-of-focus planes. However, the small energy level emitted by the fluorophore and the amplification performed by the photon detector introduces a measurement noise.

[3] Having $y(x,t_0) = y_{0,0} \exp \frac{-2x^2}{{r_0}^2}$, where r_0 is the half-width of the bleach at time $t_0 = 0$, the solution $y(x,t)$ of diffusion equation $\frac{\partial y}{\partial t} = D\frac{\partial^2 y}{\partial x^2}$ and the maximum depth at time t, i.e. $y(0,t)$ are as follows: $y(x,t) = \frac{y_{0,0} r_0}{\sqrt{{r_0}^2+8Dt}} \exp \frac{-2x^2}{{r_0}^2+8Dt}$, $y(0,t) = \frac{y_{0,0} r_0}{\sqrt{{r_0}^2+8Dt}}$. The calculation of diffusion coefficient D then resides in the weighted linear regression: a plot of $(\frac{y_{0,0}}{y(0,t)})^2$ against time should give a straight line with the tangent $\frac{8D}{{r_0}^2}$.

2. Problem formulation

2.1. Reaction-diffusion system

FRAP (Fluorescence Recovery After Photobleaching) technique is based on application of short, intense laser irradiation to a small target region of the cell that causes irreversible loss in fluorescence in this area without any damage in intracellular structures. After the "bleach" (or "bleaching"), the observed recovery in fluorescence in the "bleached area" reflects diffusion of fluorescence compounds from the area outside the bleach. For an arbitrary geometry of bleach spot and assuming (i) local homogeneity, i.e. assuring that the concentration profile of fluorescent particles is smooth, (ii) isotropy, i.e. diffusion coefficient is space-invariant, (iii) an unrestricted supply of unbleached particles outside of the target region, i.e. assuring the complete recovery,[4] the unbleached particle concentration C as a function of spatial coordinate $\vec{r}$ and time t is modeled with the following diffusion-reaction equation on two-dimensional domain Ω:

$$\frac{\partial C}{\partial t} - \nabla \cdot (D \nabla C) = R(C) \ , \tag{1}$$

where D is the fluorescent particle diffusivity within the domain Ω and $R(C)$ is a reaction term.

The initial condition and time varying Dirichlet boundary conditions are:

$$C_0 = f(\vec{r}, t_0) \ \text{ in } \Omega, \quad C(t) = g(\vec{r}, t) \text{ in } \partial\Omega \times [t_0, T]. \tag{2}$$

The reaction term $R(C)$ is often viewed as negligible under assumptions that diffusion of fluorescence compounds (proteins) is not restricted (e.g. by some binding to the medium) and that photobleaching of these molecules during recovery is negligible. In occasions where the binding reaction takes place, we can not reduce our process to the one component diffusion equation, but the dynamics of binding reaction and eventually the diffusion of bound complexes have to be modelled, see e.g. [15]. Consequently, if $R(C)$ is neglected, Eq. (1) becomes the Fickian diffusion equation. In contrast, under continual photobleaching during image acquisition, this reaction term could be described as a first order reaction: $R(C) = -k_S \, C$, where k_S is a rate constant describing bleaching during scanning [6].

It is of utmost importance to identify the relation between concentration of particles C and fluorescent signal ϕ. Although Eq. (1) and objective function J, cf. (10), works with concentrations, in fact we measure the fluorescence intensity level and not directly C. If the relation $C = k_F \phi$, where k_F is a constant, holds, than we can work with the measured signal without necessity of any recalculation. On the contrary, if k_F is space or time dependent, then we should design an experiment and estimate this dependence.

[4]The recovery is not always complete. It is usually modelled by introducing some correction term. More consistent method resides in the special time dependent Neumann boundary condition in form of a saturation curve.

Before bleaching, some number of so-called pre-bleach measurements are performed. Notice that the pre-bleach profile C_{pre} represents a steady state constant concentration profile which has to be gradually recovered for $t \to \infty$. Thereafter, based on the pre-bleach data ϕ_{pre}(e.g. its average value), we reach the coefficient k_F as follows: $k_F = \frac{C_{pre}}{\phi_{pre}}$. Consequently, in order to have experimental values C_{exp} representing the concentration profiles after bleaching, we have to divide the post-bleach fluorescence signal by its pre-bleach value, as it is explained in the following.

2.2. One-dimensional one component diffusion equation

For a linear bleach spot perpendicular to a longer axis (let this axis be denoted as r) and assuming local homogeneity and isotropy, the recovery of unbleached particle concentration as a function of spatial coordinate r and time t is modeled with a linear, diffusion-reaction equation

$$\frac{\partial C}{\partial t} - D\frac{\partial^2 C}{\partial r^2} = R(C) \ . \tag{3}$$

If we adopt the form of reaction term according to $R(C) = -k_S\, C$ and introduce the dimensionless spatial coordinate x, the dimensionless diffusion coefficient p, the dimensionless time τ and the dimensionless concentration y by

$$x := \frac{r}{L}, \quad p := \frac{D}{D_0}, \quad \tau := t\,\frac{D_0}{L^2}, \quad y := \frac{C}{C_{pre}} \ , \tag{4}$$

where L is the length of our specimen in direction perpendicular to bleach spot, D_0 is a constant with some characteristic value (unit: $\mathrm{m^2 s^{-1}}$), and C_{pre} is a pre-bleach concentration of C, we finally obtain the following form of dimensionless diffusion-reaction equation on one-dimensional domain, i.e. for $x \in [0, 1]$

$$\frac{\partial y}{\partial \tau} - p\frac{\partial^2 y}{\partial x^2} = -\frac{k_S L^2}{D_0} y \ . \tag{5}$$

The initial condition and time varying Dirichlet boundary conditions are:

$$y(x, \tau_0) = f(x), \quad x \in [0, 1], \tag{6}$$

$$y(0, \tau) = g_0(\tau), \quad y(1, \tau) = g_1(\tau), \quad \tau \geq \tau_0. \tag{7}$$

2.3. Experimentally measured data

Based on FRAP experiments, we have a 2D dataset in form of a table with experimental values $y_{exp}(r_i, t_j)$ (already normalized), where $(N+1)$ rows correspond to the number of spatial points where the values are measured, and $(m^* + M + 1)$ columns correspond to the number of discrete time points, i.e. time instant when the data were measured:

$$y_{exp}(r_i, t_j),\ i = 0 \ldots N,\ j = -m^* \ldots M. \tag{8}$$

This can be read by columns as the concentration profiles (along r axis) in m^*+M+1 discrete time points, where m^* corresponds to the number of columns with pre-bleach data containing the information about the steady state and optical distortion, and $M+1$ columns of post-bleach data contain the information about the transport of unbleached particles (due to the diffusion process) through the boundary of bleach spot (our computational domain Ω).

The row data are further re-scaled in order to be in the following form:

$$y_{exp}(x_i, \tau_j),\ i = 0 \dots n,\ j = -m^* \dots m, \tag{9}$$

where space interval between first and last measurement points we take into account is chosen as $[a, b]$. Thus, $L = b - a$ is the length of space interval in physical units, i.e. [m], chosen by the person performing the measurment. The re-scaled dimensionless space interval is again $x \in [0, 1]$ and the re-scaled distance between two space measurements is $h = \frac{1}{n}$. Time interval between two measurements is T in [s], re-scaled dimensionless time interval is $\tau_t = \frac{TD_0}{L^2}$. For the further calculation, the number of post-bleach measurements can be also reduced, i.e. let $m \leq M$. Recall that τ_0 corresponds to the first post-bleach measurement, and $x_0 = 0$, $x_n = 1$. Consequently, $y_{exp}(x_i, \tau_0),\ i = 0 \dots n$, represent the initial condition and $y_{exp}(0, \tau_j)$ and $y_{exp}(1, \tau_j),\ j = 0 \dots m$, the left and right Dirichlet boundary conditions, respectively.

Recall that due to the measurement noise both the respective $j - profiles$ $y_{exp}(x_i, \tau_j),\ i = 0 \dots n$, and the initial and boundary conditions cannot be simply approximated by a smooth function. The forthcoming task is to analyze the measurement noise from real data and to treat it correctly, i.e. to use it for the setting of the regularization parameter, see the following section 3.

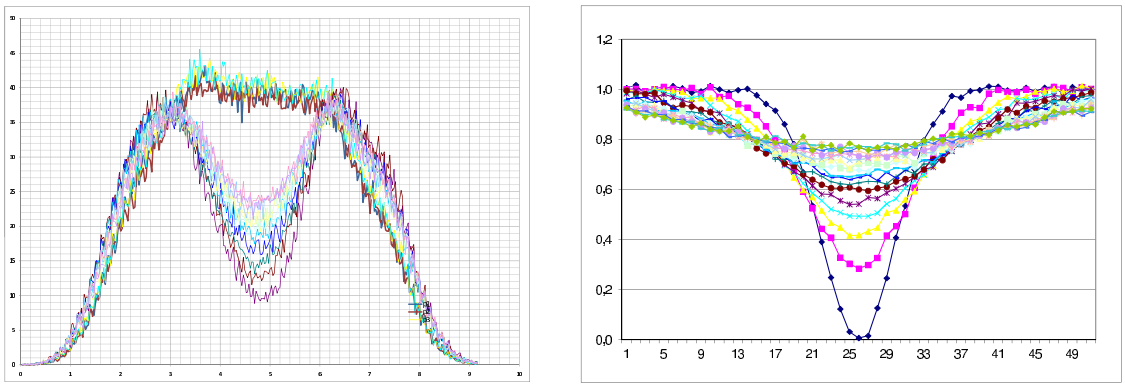

Figure 1: Left: Experimental data from FRAP experiments with red algae *Porphyridium cruentum* describing the phycobilisomes mobility on thylakoid membrane [7]. Right: Synthetic data used for numerical experiments. The y-axis represents the dimensionless concentration and x-axis the spatial coordinate, both in arbitrary units.

3. Inverse problem and its regularization

3.1. Determination of diffusivity as a parameter estimation problem

The problem of autofluorescence compound (e.g. phycobilisomes) diffusivity determination based on time series of FRAP experimental data will be further formulated as a parameter estimation problem. We construct an objective function J representing the disparity between the experimental and simulated time-varying concentration profiles, and then within a suitable method we look for such a value p minimizing J. The usual form of an objective function is the sum of squared differences between the experimentally measured and numerically simulated time-varying concentration profiles:

$$J(p) = \sum_{j=0}^{m} \sum_{i=0}^{n} \left[y_{exp}(x_i, \tau_j) - y_{sim}(x_i, \tau_j) \right]^2 \ , \tag{10}$$

where $y_{sim}(x_i, \tau_j)$ are simulated values resulting from the solution of PDE (5) with the initial and boundary conditions (6)-(7) for the known parameter p, which is now the independent variable, i.e. $y_{sim} = y_{sim}(p)$. For the sake of clarity we further neglect the other parameter concerning the reaction term, i.e. we neglect the influence of bleaching during scanning, i.e. we put $\frac{k_S L^2}{D_0} = 0$.

Taking into account the biological reality residing in possible time dependence of phycobilisomes diffusivity, we further consider two cases:

1. First, we can take both sums for i and j in (10) together. In this case, the scalar p^* is a result of a minimization problem $p^* = \arg\min_p J(p)$.

2. Secondly, we can consider each j-th time instant separately. In this case, the m solutions $p_1^*, \ldots, p_m^*$ with values $J_1, \ldots, J_m$ correspond to each minimization problem for fixed j in sum (10), i.e. ${p_j}^* = \arg\min_{p_j} J_j(p_j)$, where $J_j(p_j) = \sum_{i=0}^{n} \left[y_{exp}(x_i, \tau_j) - y_{sim}(x_i, \tau_j, p_j) \right]^2$, and we have a "dynamics" of diffusivity p evolution.

Our problem is ill-posed in the sense that the solution, i.e. the diffusion coefficients $D_j = p_j \ D_0, \ j = 1, \ldots, m$, does not depend continuously on the data and may be very sensitive to noise. This led us to the necessity of some stabilizing procedure[5] and the formulation of another cost function by adding the regularization term $\alpha ||p - p_{reg}||^2$ to (10), see [3, 5, 17]. Here $\alpha \geq 0$ is a regularization parameter and p_{reg} is an expected regularized value. Doing this, we use an apriori information about the solution, in other words we assume that $p \equiv p(x, \tau)$ is almost constant with respect to x and τ and regularization term moves the minimum of functional $J(p) = \sum_{j=1}^{m} J_j(p_j)$, i.e. the solutions $p_1^*, \ldots, p_m^*$ towards a constant. In case $\alpha \to \infty$

[5]The "naive approach" consisting in the hope that the typical oscillation of ${p_j}^*$ can be suppressed by removing the noise from data, e.g. by smoothing using the Fourier transformation, was treated in [12] and further abandoned by the authors.

we obtain $p_j^* = p_{reg}, j = 1, \ldots, m$. Note that taking $\alpha = 0$, the regularization term vanishes, i.e. the functional (10) is the special case of a more general functional, see the next section.

3.2. Three types of optimization problem

Define the cost functions

$$J_j(p_j, \alpha) = \sum_{i=0}^{n} \left[y_{exp}(x_i, \tau_j) - y_{sim}(x_i, \tau_j, p_j)\right]^2 + \alpha \left(p_j - p_{reg}\right)^2, \quad j = 1, \ldots, m, \quad (11)$$

$$J(p_1, \ldots, p_m, \alpha) = \sum_{j=1}^{m} J_j(p_j, \alpha). \quad (12)$$

Three types of a one-dimensional optimization problem are considered:

1. Scalar p is a solution when taking both sums for i and j in together:

$$p^* = \arg\min_{p} \sum_{j=1}^{m} \sum_{i=0}^{n} \left[y_{exp}(x_i, \tau_j) - y_{sim}(x_i, \tau_j, p)\right]^2 \quad (13)$$

2. Each j^{th} time instant separately without regularization ($\alpha = 0$):

$$p_j^* = \arg\min_{p_j} \sum_{i=0}^{n} \left[y_{exp}(x_i, \tau_j) - y_{sim}(x_i, \tau_j, p_j)\right]^2 \quad (14)$$

3. Each j^{th} time instant separately using so-called Tikhonov regularization:

$$p_j^*(\alpha) = \arg\min_{p_j, p_{reg}} \left\{ \sum_{i=0}^{n} \left[y_{exp}(x_i, \tau_j) - y_{sim}(x_i, \tau_j, p_j)\right]^2 + \alpha \left(p_j - p_{reg}\right)^2 \right\} \quad (15)$$

We use a basic optimization method leading to values p^*, p_j^*, $p_j^*(\alpha)$ that minimize respective cost functional. Values p_j^*, $p_j^*(\alpha)$ are approximations of diffusion coefficients. We briefly describe a basic optimization method without loss of generality for the case of solving problem (13).

Basic optimization method is an iteration process starting from an initial point $p^{(0)}$ and generating a sequence of iterates $p^{(1)}, p^{(2)}, \ldots$ leading to a value p^* such that

$$p^{(l+1)} = p^{(l)} + \sigma^{(l)} d^{(l)},$$

where

- $d^{(l)}$ is a direction vector determined on the basis of values

$$p^{(j)},\ J(p^{(j)}),\ J'(p^{(j)}),\ J''(p^{(j)}), \quad 0 \le j \le l,$$

- $\sigma^{(l)} > 0$ is a step-length determined on the basis of behavior of the function J in the neighborhood of $p^{(l)}$.

There exist several methods for determination of direction vector and step-length selection (line-search or trust-region method) described e.g. in [11]. The trust-region method, implemented in the system for universal functional optimization [8], was used in our numerical test described in the next section.

3.3. Implementation

In this subsection we describe how we implemented both the direct problem, i.e. solution of problem (5)-(7), and the parameter estimation problem, i.e. minimization of a respective functional J.

In order to compute a function value $J_j(p_j^{(l)}, \alpha)$ in (12) for a given $p_j^{(l)}$ in the l^{th} iteration, we need to know both

- the experimental values $y_{exp}(x_i, \tau_j),\ i = 0 \dots n,\ j = 0 \dots m$,
- the simulated values $y_{sim}(x_i, \tau_j, p_j^{(l)}),\ i = 0 \dots n,\ j = 0 \dots m$.

It means that in each l^{th} iteration we need to solve the problem (we use the notation $y_{sim} \equiv y,\ p_j^{(l)} \equiv p$ for simplicity)

$$\frac{\partial y}{\partial \tau} - p\,\frac{\partial^2 y}{\partial x^2} = 0\ , \tag{16}$$

with the initial and boundary conditions defined by the experimental data

$$y(x, \tau_0, p) = y_{exp}(x, \tau_0) \quad \text{for} \quad x \in [0, 1], \tag{17}$$

$$y(0, \tau, p) = y_{exp}(0, \tau), \quad y(1, \tau, p) = y_{exp}(1, \tau) \quad \text{for} \quad \tau \geq \tau_0. \tag{18}$$

Problem (16)-(18) for simulated data $y(x_i, \tau_j, p_j)$ was solved numerically using two following finite difference schemes [2] for uniformly distributed nodes with the space steplength Δh and the variable time steplength $\Delta\tau$:

- The explicit scheme of order $\Delta\tau + \Delta h^2$:

$$y_{i,j} = \beta y_{i-1,j-1} + (1 - 2\beta) y_{i,j-1} + \beta y_{i+1,j-1}$$

- The Crank-Nicholson implicit (CN) scheme of order $\Delta\tau^2 + \Delta h^2$:

$$-\frac{\beta}{2} y_{i-1,j} + (1 + \beta) y_{i,j} - \frac{\beta}{2} y_{i+1,j} = \frac{\beta}{2} y_{i-1,j-1} + (1 - \beta) y_{i,j-1} + \frac{\beta}{2} y_{i+1,j-1}$$

Here $\beta = \frac{\Delta\tau}{\Delta h^2}\, p$ and $y_{i,j} \equiv y(x_i, \tau_j, p_j)$ are the computed values in nodes that enter the function J as values $y_{sim}(x_i, \tau_j, p_j)$. Recall that for the explicit scheme the condition $\beta \leq 1/2$ must hold.

Concerning the steplengths used in the numerical schemes, we set the space steplength to be $\Delta h = 1/n$ (smaller splitting $\Delta h = 1/(\kappa_s n)$ with $\kappa_s \in \mathcal{N}$ can also be considered). The time steplength $\Delta\tau$ is variable but should be ideally of the same order as Δh^2 (or Δh in the CN scheme) and in the explicit scheme has to fulfill the relation $\Delta\tau \leq \frac{\Delta h^2}{2p}$. In order to get from the $(j-1)$-th time instant to the j-th, we need to perform $\kappa_t = \lceil \frac{TD_0}{L^2 \Delta\tau} \rceil$ substeps of the above chosen scheme, where $\kappa_t \in \mathcal{N}$ is the smallest integer that is not less than $\frac{TD_0}{L^2 \Delta\tau}$.

4. Numerical simulation results

We have performed numerical experiments with the synthetic data corrupted by the 10% Gaussian noise with $n = 51$, $m = 19$ and consider each j-th time instant separately, i.e. j is fixed in sum (12). We report the results using the CN scheme (they are in fact independent of the used scheme) and illustrate the difficulties caused by the ill-posedness of our problem.

In Figure 2 we can see big jumps in computed approximated values $p_j^*, j=1,\dots,m$ when using no regularization ($\alpha = 0$). In contrast, regularization technique ($\alpha > 0$) seems to cope with ill-posedness quite well. The solutions $p_1^*(\alpha),\dots,p_m^*(\alpha)$ become smoother and tend to the estimated regularized value p_{reg} for larger α (larger weight of the regularization term). The regularized value corresponds to the exact solution $1/\pi \approx 0.3183$.

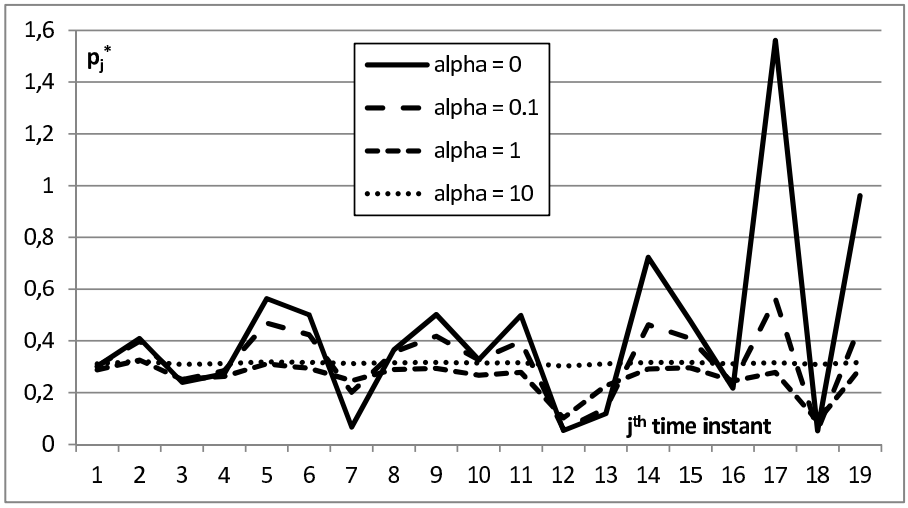

Figure 2: Dimensionless diffusivities $p_j^* = \frac{D_j}{D_0}$: Values $p_1^*(\alpha),\dots,p_{19}^*(\alpha)$.

When using this approach, the variance of solutions $p_j^*(\alpha)$ tends to zero for $\alpha \to \infty$, i.e. $p_j^*(\alpha) \to p_{reg}\ \forall j = 1,\dots,m$, but the function values $J(p^*,\alpha)$, see (12), become larger (however there is a supremum). This fact is demonstrated in Figure 3, where we have used relative deviation from the average value (coefficient of variation[6]) as a solution norm:

$$c_v(\alpha) = \frac{1}{m\, \emptyset p_j^*(\alpha)} \sqrt{\sum_{j=1}^{m} [p_j^*(\alpha) - \emptyset p_j^*(\alpha)]^2}. \tag{19}$$

A proper choice of the regularization parameter α balances the above types of the curves. One of the possible criteria how to choose a proper α which is in some sense

[6]The coefficient of variation (c_v) is defined as the ratio of the standard deviation to the mean $c_v = \frac{\sigma}{\mu}$, which is the inverse of the signal-to-noise ratio.

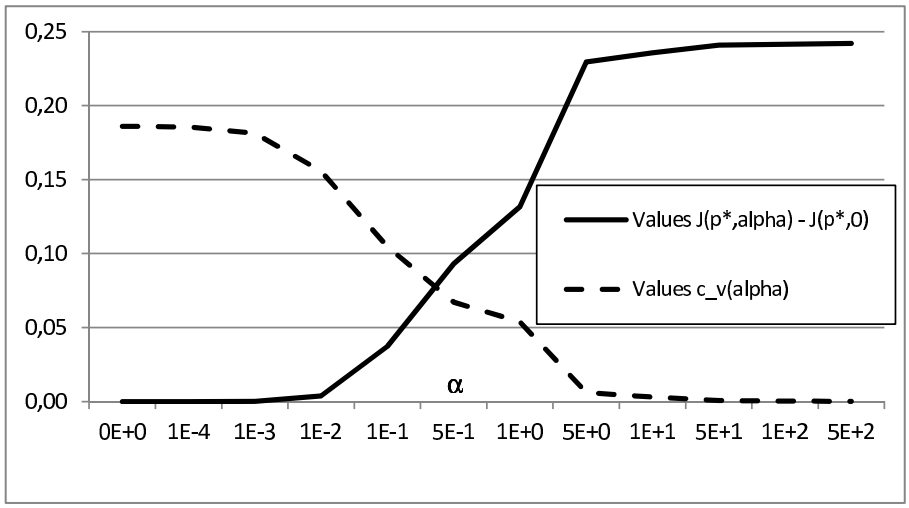

Figure 3: Values $J(p^*, \alpha) - J(p^*, 0)$ are increasing, values $c_v(\alpha)$ are decreasing.

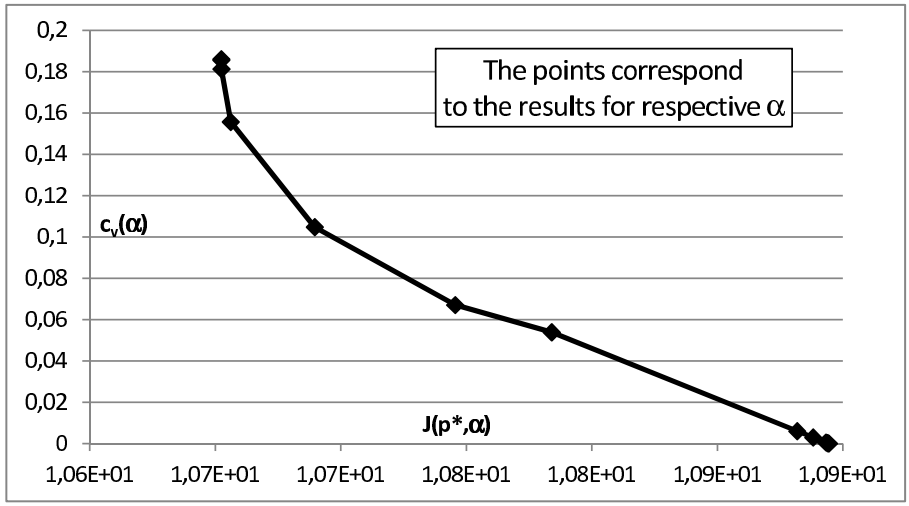

Figure 4: The L-curve – values $J(p^*, \alpha)$, see (12), against values $c_v(\alpha)$, see (19).

optimal is called the L-curve. We plot the value of objective function J against the value $c_v(\alpha)$. The *L-curve-optimal* parameter α^* usually corresponds to the point with maximal curvature. In Figure 4, we plot the L-curve resulting from our numerical tests for the 10% Gaussian noise, i.e. for $c_v = 0.1$. We see that for our "FRAP problem" and a particular noise level, there is not a sharp corner. Furthermore, the question of *optimal* value of α^* may also depend on what the user expects or prefers, if rather small function value $J(p^*, \alpha)$ or more constant solutions $p_1^*, \ldots, p_m^*$, i.e. small value $c_v(\alpha)$, see e.g. [4].

5. Conclusions

The purpose of this paper was to present the real problem residing in the estimation of diffusivity of phycobilisomes on thylakoid membrane based on spatio-temporal FRAP images. While the state-of-the-art methods in FRAP measurement of photosynthetic complexes mobility are usually based on the curve fitting to an analytical (closed form) models, which need some unrealistic conditions to be supposed, our method is based on finite difference approximation of diffusion process and on the minimization of an objective function evaluating both the disparity between the experimental and simulated time-varying concentration profiles and the smoothness of the time evolution of diffusivity. This approach naturally takes into account the time-dependent Dirichlet boundary conditions and can include also a reaction term (e.g. modeling the low level bleaching during scanning) and the time varying fluorescence signal as well.

Our program *CA-FRAP 4.0* is actually under testing, however, for the previously known diffusion coefficient and the synthetic data corrupted by the Gaussian noise it computes satisfactory results. Afterward, we determined the diffusivities for the real data of FRAP measurements (with the red algae *Porphyridium cruentum*). The range of result $10^{-15}\mathrm{m}^2\mathrm{s}^{-1}$ ($10^{-3}\mu\mathrm{m}^2\mathrm{s}^{-1}$) is in agreement with reference values.

Acknowledgements

This work was supported by the project Jihočeské výzkumné centrum akvakultury a biodiverzity hydrocenóz (CENAKVA CZ.1.05/2.1.00/01.0024), OP VaVpI and by the long-term strategic development financing of the Institute of Computer Science (RVO:67985807).

References

[1] Axelrod D., Koppel D. E., Schlessinger J., Elson E., and Webb W. W.: Mobility measurement by analysis of fluorescence photobleaching recovery kinetics. Biophys. J. **16** (1976), 1055–1069.

[2] Babuška I., Práger M., and Vitásek E.: *Numerical processes in differential equations*. John Wiley & Sons, London, 1966.

[3] Chavent G. and Kunish K.: Regularization in state space. Mathematical Modelling and Numerical Analysis **27** (1995), 535–556.

[4] Engl W. and Grever W.: Using the *L*-curve for determining optimal regularization parameter. Numer. Math. **69** (1994), 25-31.

[5] Hinestroza D., Murio D. A., and Zhan S.: Regularization techniques for nonlinear problems. Comput. Math. Appl. **37** (1999), 145–159.

[6] Irrechukwu O. N. and Levenston M. E.: Improved estimation of solute diffusivity through numerical analysis of FRAP experiments. Cellular and Molecular Bioengineering **2** (2009), 104-117.

[7] Kaňa R., Prášil O., and Mullineaux C. W.: Immobility of phycobilins in the thylakoid lumen of a cryptophyte suggests that protein diffusion in the lumen is very restricted. FEBS letters **583** (2009), 670-674.

[8] Lukšan L., Tůma M., Vlček J., Ramešová N., Šiška M., Hartman J., and Matonoha C.: UFO 2011 – Interactive system for universal functional optimization. Technical Report V-1151, Institute of Computer Science, Academy of Sciences of the Czech Republic, Prague 2011 (`http://www.cs.cas.cz/luksan/ufo.html`).

[9] Mueller F., Mazza D., Stasevich T. J., and McNally J. G.: FRAP and kinetic modeling in the analysis of nuclear protein dynamics: what do we really know?. Current Opinion in Cell Biology **22** (2010), 1-9.

[10] Mullineaux C. W., Tobin M. J., and Jones G. R.: Mobility of photosynthetic complexes in thylakoid membranes. Nature **390** (1997), 421-424.

[11] Nocedal J. and Wright S. J.: *Numerical optimization, second edition.* Springer, New York, 2006.

[12] Papáček Š., Kaňa R., and Matonoha C.: Estimation of diffusivity of phycobilisomes on thylakoid membrane based on spatio-temporal FRAP images. Math. Compt. Modelling (2012), doi:10.1016/j.mcm.2011.12.029.

[13] Papáček Š. and Matonoha C.: Error analysis of three methods for the parameter estimation problem based on spatio-temporal FRAP measurement. SNA 2013, submitted.

[14] Sbalzarini I. F.: Analysis, modeling and simulation of diffusion processes in cell biology. VDM Verlag Dr. Muller, 2009.

[15] Sprague B. L., Pego R. L., Stavreva D. A., and McNally J. G.: Analysis of binding reactions by fluorescence recovery after photobleaching. Biophysical Journal. **86** (2004), 3473–3495.

[16] Thomas J. and Webb W. W.: Fluorescence photobleaching recovery: a probe of membrane dynamics. In: S. Grinstein and K. Foskett (Eds.), *Non-Invasive Techniques in Cell Biology*, pp. 129–152. Wiley-Liss, Inc., 1990.

[17] Tychonoff A. N. and Arsenin V. Y.: *Solution of Ill-posed problems.* Washington, Winston & Sons, 1977.